Appl. Chem. Eng., Vol. 34, No. 6, December 2023, 633-639
https://doi.org/10.14478/ace.2023.1083

Article

Strategies to Design Efficient Donor-Acceptor (D-A) Type Emitting Molecules: Molecular Symmetry and Electron Accepting Ability of D-A Type Molecules

Hyun Gi Kim[*,**,***], **Young-Seok Baek**[*], **Sung Soo Kim**[*,**,***], **Sang Hyun Paek**[*,**,***] and **Young Chul Kim**[*,**,***,†]

[*]*Department of Chemical Engineering, Kyung Hee University, Yongin-si 17104, Korea*
[**]*Core Facility Center for Analysis of Optoelectronic Materials and Devices, Kyung Hee University, Yongin-si 17104, Korea*
[***]*Regional Innovation Center for Components and Materials for Information Display, Kyung Hee University, Yongin-si 17104, Korea*
(Received September 20, 2023; Revised October 18, 2023; Accepted October 18, 2023)

Abstract

We synthesized 2-(10-methyl-10H-phenothiazin-3-yl)-5-phenyl-1,3,4-oxadiazole (MPPO) and 5,5-(10-methyl-10H-phenothiazin-3,7-diyl)-bis-(2-phenyl-1,3,4-oxadiazole) (DPPO). MPPO has both electron-donating and electron-accepting substituents with asymmetric molecular geometry. By incorporating one extra electron-accepting group into MPPO, we created a symmetric molecule, which is DPPO. The optical and electrochemical properties of these compounds were measured. The lowest unoccupied molecular orbital (LUMO) level of DPPO was lower than that of MPPO. The excited-state dipole moment of DPPO, with symmetric geometry, was calculated to be 4.1 Debye, whereas MPPO, with asymmetric geometry, had a value of 7.0 Debye. The charge-carrier mobility of both compounds was similar. We fabricated non-doped organic light-emitting diodes (OLEDs) using D-A type molecules as an emitting layer. The current efficiency of the DPPO-based device was 7.8 cd/A, and the external quantum efficiency was 2.4% at 100 cd/m^2, demonstrating significantly improved performance compared to the MPPO-based device. The photophysical and electroluminescence (EL) characteristics of the two D-A type molecules showed that molecular symmetry, as well as the lowered LUMO level of DPPO, played critical roles in the enhancement of EL performance.

Keywords: *Phenothiazine, Oxadiazole, Donor-acceptor type molecule, Molecular symmetry, Organic light-emitting diode*

1. Introduction

Organic electroluminescent materials composed of electron donor and acceptor (D-A) groups have been extensively explored by numerous researchers. This is due to their high bipolar charge-carrier transport mobility[1,2], and they have demonstrated immense potential for various optoelectronic devices, such as solar cells[3], thin-film transistors (TFTs)[4], and organic light-emitting diodes (OLEDs)[5,6]. The bipolar charge-transporting nature of D-A type molecules can yield high solid-state photoluminescence (PL) quantum yields, offering the potential to enhance the electroluminescence (EL) performance and operational stability in OLEDs[7,8]. Additionally, D-A type molecules have an advantage in that their emission characteristics can be easily modified through a thoughtful choice of the D and A moieties[7]. Studies on D-A structures have been conducted for various purposes over the past few decades. Tian's group synthesized a symmetric D-A-D molecule, 2-{2,6-bis-[2-(4-diphenylamino-phenyl)-vinyl]-pyran-4-ylidene}-malononitrile (DADP), as a material for solar cells[9]. They reported that the combination of the electron-accepting group and the electron-donating group with a shorter π-spacer offers the advantage of high hole mobility for applications in solar cells. A study on the molecular symmetry of D-A type molecules has shown that host materials with an asymmetric molecular structure are more beneficial for transporting charge carriers than those with a symmetric one[10]. Additionally, there is research on D-A type molecules as thermally activated delayed fluorescence (TADF) emitters. According to Lee *et al.*[11], the strong electron-donating and electron-accepting abilities, along with the large dihedral angle, help D-A type TADF emitters reduce the overlap between the highest occupied molecular orbital (HOMO) and lowest unoccupied molecular orbital (LUMO), enabling high quantum yields in resulting devices. Li and his co-workers designed and synthesized symmetric emitters with common vertical transition paths and those with more severe non-radiative pathways dominating the transition process[12]. However, the effects of molecular symmetry on the electroluminescence (EL) characteristics of D-A and D-A-D type emitting materials have not been generally understood.

In this work, we report the synthesis and characterization of new fluorescent materials, which are commonly based on the phenothiazine electron donor and the oxadiazole acceptor. Specifically, we discuss two types of materials: D-A type and A-D-A type, featuring 2-(10-methyl-10H-phenothiazin-3-yl)-5-phenyl-1,3,4-oxadiazole (MPPO) and 5,5-(10-methyl-10H-phenothiazin-3,7-diyl)-bis-(2-phenyl-1,3,4-oxadiazole) (DPPO) as the key components. The phenothiazine group possesses an

† Corresponding Author: Kyung Hee University
Department of Chemical Engineering, Yongin-si 17104, Korea
Tel: +82-31-201-3736 e-mail: kimyc@khu.ac.kr

pISSN: 1225-0112 eISSN: 2288-4505

excellent electron-donating property, leading to the formation of stable radical cations[13]. Additionally, it has a non-planar geometry with a folding angle along the N-S axis, which varies depending on the size, nature, and position of substituents[14-16]. This non-planar geometry helps to reduce the extent of intermolecular π-π stacking and concentration quenching in OLEDs. By incorporating the phenothiazine electron-donating group in combination with the 1,3,4-oxadiazole group, known for its electron-accepting ability[17,18], both MPPO and DPPO are expected to exhibit bipolar charge-carrier transport characteristics and serve as recombination sites. Most D-A type molecules are known to exhibit intramolecular charge transfer (ICT) characteristics, involving rapid intramolecular electron transfer from the donor to the acceptor[19]. Furthermore, the extent of ICT in fluorescent D-A molecules tends to vary with their molecular symmetry, affecting both their electron-accepting ability and electroluminescence (EL) performance[20,21]. Therefore, we conducted an investigation into the ICT characteristics of the asymmetric D-A type molecule, MPPO, and the symmetric A-D-A type molecule, DPPO. We also explored the impact of molecular symmetry on the EL performance of these fluorescent D-A molecules.

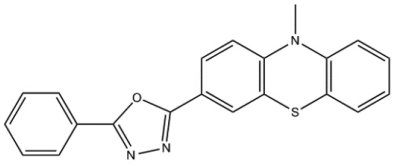

MPPO

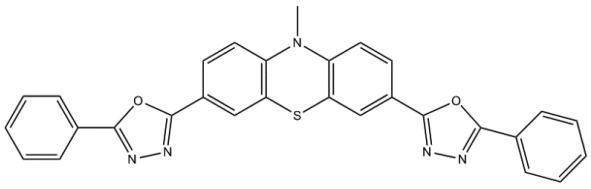

DPPO

Figure 1. Molecular structures of the D-A type molecules.

2. Experimentals

2.1. Synthesis

New green-emitting materials, 2-(10-methyl-10H-phenothiazin-3-yl)-5-phenyl-1,3,4-oxadiazole (MPPO) and 5,5-(10-methyl-10H-phenothiazin-3,7-diyl)-bis-(2-phenyl-1,3,4-oxadiazole) (DPPO), as depicted in Figure 1, were synthesized. The process involved the preparation of 10-methylphenothiazine with a 92% yield through the methylation of phenothiazine. Subsequently, 10-methyl-phenothiazine-3-carbaldehyde was synthesized by substituting one formyl group using the Vilsmeier-Haak reaction[22,23]. Finally, in-situ oxidative cyclization occurred after imination of 10-methyl-phenothiazine-3-carbaldehyde with benzohydrazide, resulting in an 89% yield of MPPO. MPPO was analyzed using 1H NMR and 13C NMR spectroscopy on a Jeol JNM-AL300 FT-NMR spectrometer operating at 300 MHz. Chemical shifts (multiplicity, coupling constant (Hz), integrated values) were referenced to tetramethylsilane (TMS). High-resolution mass spectra were recorded on a JEOL JMS-700 spectrometer. Mp. 156~158 °C; 1H NMR (300 MHz, CDCl3): δ 8.11~8.15 (m, 2H), 7.93~7.97 (dd, J1 = 8.43 Hz, J2 = 1.83 Hz, 1H), 7.87 (d, J = 1.83 Hz, 1H), 7.51~7.55 (m, 3H), 7.16~7.26 (m, 2H), 6.99 (t, J = 7.50 Hz, 1H), 6.85~6.92 (m, 2H), 3.45 (s, 3H); 13C NMR (300 MHz, CDCl3): δ 164.22, 164.07, 148.71, 144.64, 131.59, 129.06, 127.77, 127.31, 126.86, 126.60, 125.32, 124.29, 124.03, 123.29, 122.54, 117.95, 114.55, 114.12, 35.61. EI-HRMS (70 eV, EI+) m/z calcd for $C_{21}H_{15}N_3OS$: C, 70.57; H, 4.23, found: C, 70.36; H, 4.16.

2.2. Materials characterization

The thermal properties of the emitting materials were characterized through thermogravimetric analysis (TGA) using an SDT Q600 instrument from TA Instruments and differential scanning calorimetry (DSC) with a DSC N536-0003 device from PerkinElmer. The measurements were conducted at a scan rate of 10 °C/min under a nitrogen atmosphere. UV-visible absorption and photoluminescence (PL) spectra were recorded using an Agilent 8453 spectrophotometer and a PTI QM-4 spectrofluorometer, respectively. The electrochemical properties of the materials were assessed via cyclic voltammetry. This analysis was carried out using an eDAQ e-corder 401 instrument in nitrogen-purged dichloromethane (DCM), which contained 0.1 M tetrabutylammonium hexafluorophosphate (TBAPF6) as a supporting electrolyte. The measurements were conducted at a scan rate of 50 mV/s. For this analysis, a glassy carbon working electrode, a platinum auxiliary electrode, and a saturated Ag/AgCl reference electrode were employed, with potentials referenced against ferrocene.

2.3. OLED fabrication and characterization

Indium tin oxide (ITO) coated glass substrates with a surface resistance of 10 Ω/□ were patterned through photolithography and underwent a cleaning process involving successive ultrasonication in trichloroethylene, acetone, ethanol, deionized water, and isopropyl alcohol. Subsequently, they were dried in a convection oven at 120 °C. Oxygen plasma treatment was applied to the ITO substrates to enhance the interfacial adhesion between the substrate and the organic layer. All the organic and cathode metal layers were deposited using thermal evaporation under a vacuum of approximately ~3 × 10^{-6} torr. The deposition rates were 1.0, 0.1, and 3~4 Å/s for the organic, LiF, and Al layers, respectively. The current density-voltage-luminance (J-V-L) characteristics and electroluminescence (EL) spectra of the OLED devices were measured with a M6100 OLED IVL Test System equipped with a Keithley 236 source/measure unit.

3. Results and discussion

3.1. Thermal properties

We examined the thermal stability of the D-A type molecules prior to the OLED fabrication process, which involved successive thermal evaporation. The thermal decomposition temperature (T_d), crystal-

Table 1. Physical Properties of the Compounds

	T_m/T_d[a] (°C)	Film λ_{ab} (nm)	Film λ_{em} (nm)	HOMO[b] (eV)	LUMO[c] (eV)
MPPO	158 / 255	285, 380	499	5.2	2.2
DPPO	276 / 338	298, 396	513	5.3	2.5

[a] the temperature for 1% weight loss of the materials
[b] estimated based on CV data
[c] determined from the equation LUMO = HOMO + Eg, where Eg was calaulated from the absorption onset of the solid film.

lization temperature (T_c), and melting temperature (T_m) were measured through TGA and DSC and are summarized in Table 1. The thermal decomposition temperatures of MPPO and DPPO, defined as the temperature at which the weight loss reached 1.0%, were 255 and 338 °C, respectively. Both compounds did not exhibit cold crystallization during the DSC heating scan and displayed a single melting peak at 158 and 276 °C for MPPO and DPPO, respectively. The incorporation of the oxadiazole moiety into MPPO significantly raised both T_d and T_m, resulting in the enhanced thermal stability of DPPO. Both MPPO and DPPO exhibited sufficient thermal stability, ensuring that they would not be affected by the thermal evaporation process or by the device heating during operation.

3.2. Photophysical properties and solvatochromism

We measured the UV-vis absorption spectra of MPPO and DPPO when dissolved in organic solvents with varying polarities. As depicted in Figure 2(a) and 2(b), both compounds exhibit two absorption bands: a higher energy absorption band peaking at around 300 nm and a lower energy absorption band at approximately 350 or 380 nm. Previous reports have indicated that the phenothiazine group absorbs at around 310 nm, while the 1,3,4-oxadiazole group absorbs at around 350 nm[24,25]. The higher energy absorption band observed in both compounds is attributed to the n-π^* transition of the phenothiazine group[26], while the broader lower energy band originates from a charge-transfer (CT) complex[27,28]. Small shifts in the peak positions of the lower energy band occur because the ground-state dipole moment varies in different solvents[28]. The energy level of this CT absorption can be approximated by subtracting the electron affinity of the acceptor orbital from the ionization potential of the donor orbital[29, 30]. In contrast, the higher energy absorption band is commonly referred to as the locally-excited (LE) band, and the difference between the electron affinity and ionization potential of a donor can be estimated from the absorption wavelength.

As shown in Figure 2(c) and 2(d), we also observed significant red-shifts in the photoluminescence (PL) spectra of the compounds when dissolved in polar solvents. The emission peak wavelength of MPPO shifted from 456 nm in cyclohexane to 506 nm in N,N-Dimethylformamide (DMF). Similarly, the PL peak of MPPO, which appeared at 475 nm in cyclohexane, shifted to 506 nm in DMF, as summarized in Table 2. This indicates that the excited-state dipole moment of MPPO is larger than that of DPPO. To gain further insight into intermolecular charge transfer (ICT), we estimated the polarity

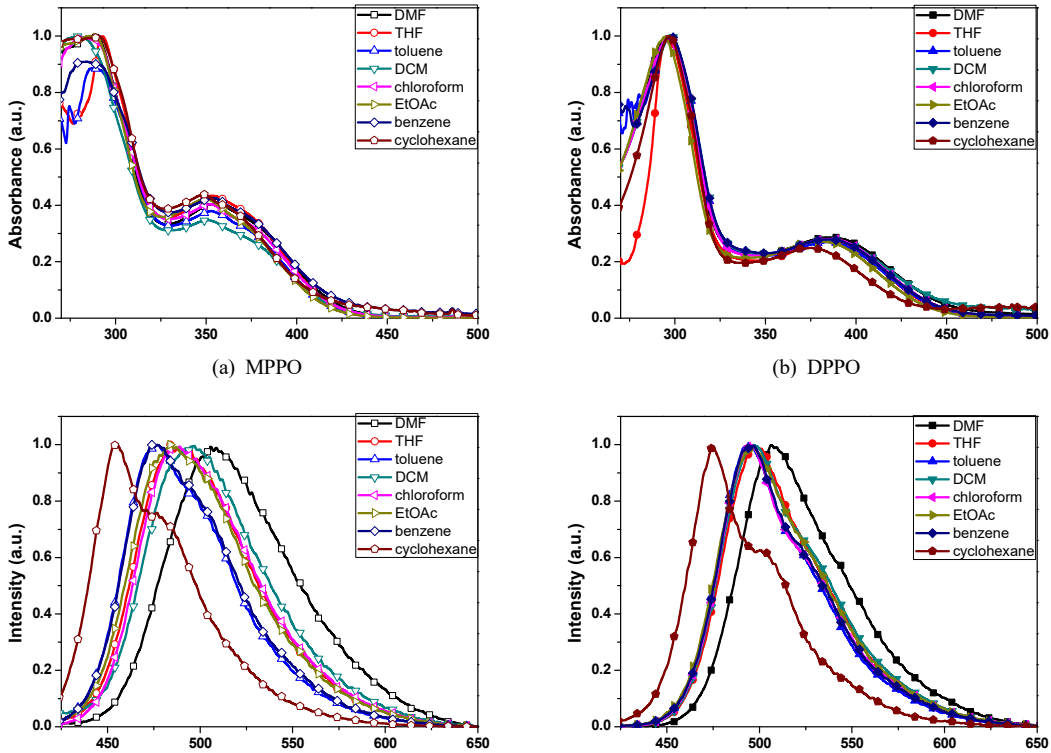

Figure 2. UV and PL emission spectra of (a) MPPO and (b) DPPO in solvents of varying polarity.

Table 2. Solvatochromism Results of the Compounds

	$\triangle f$	λ_{ab} (nm)	λ_{em} (nm)	$\triangle \nu$ (cm^{-1})
MPPO				
toluene	0.014	287, 353	476	7320
THF	0.210	293, 354	484	7587
DCM	0.218	280, 351	497	8369
DMF	0.275	286, 355	506	8406
Chloroform	0.146	284, 352	489	7959
EtOAc	0.199	285, 349	484	7992
Benzene	0.003	284, 353	477	7364
Cyclohexane	0.001	291, 349	456	6724
DPPO				
toluene	0.014	297, 383	495	5908
THF	0.210	296, 384	497	5921
DCM	0.218	297, 387	497	5719
DMF	0.275	296, 384	506	6279
Chloroform	0.146	294, 386	496	5746
EtOAc	0.199	294, 380	497	6195
Benzene	0.003	297, 384	497	5921
Cyclohexane	0.001	295, 385	475	4921

$\triangle f$: solvent polarity parameter, $\triangle \nu$: stokes shift

changes between the ground state and the excited state using the Lippert-Mataga equation[31,32]. This equation describes the relationship between the Stokes shift and solvent polarity as follows:

$$\triangle \nu = \frac{2\triangle \mu^2}{a^3 hc} f(\varepsilon, n) + const. \quad (1)$$

$$f(\varepsilon, n) = \frac{\varepsilon - 1}{2\varepsilon + 1} - \frac{n^2 - 1}{2n^2 + 1} \quad (2)$$

where $\triangle \nu = \nu_a^0 - \nu_f^0$ corresponds to the Stoke shifts, $\triangle \mu$ is the differences between the excited- and ground-state dipole moments ($\mu_e - \mu_g$), α is the solvent Onsager cavity radius, h is Plank's constant, c is the velocity of light, and ε and n are the dielectric constant and the refractive index of the solvent, respectively. f is the orientational polarizability of the solvent and the values of each solvent were adapted from the literature[33,34]. μ_g and α were calculated from the optimized structure obtained with a density functional theory (DFT) minimization using the Gaussian 09 (B3LYP functional using 6-31G-(d,p) orbital base)[35]. The Onsager cavity radius, α was determined as the distance between the donating nitrogen atom and accepting oxygen atom, corresponding to the longest distance across the molecule where charge separation can occur[35,36]. The 'a' value was calculated to be 3.24 Å for both compounds, and μ_i was 3.3 and 2.5 D for MPPO and DPPO, respectively. In Figure 3, we plotted the Stokes shift as a function of solvent polarity for both compounds. The $\triangle \mu$ values estimated from the slopes were 3.7 and 1.6 D for MPPO and DPPO, respectively, as summarized in Table 3. This result suggests that the asymmetric D-A type molecule, MPPO, possesses stronger polarity in the excited state than the symmetric A-D-A type DPPO. The significant $\triangle \mu$ can lead to a lower quantum yield of emitting materials, following Fermi's Golden Rules[31,37]. Therefore, we can anticipate that the OLED device with the DPPO emitting layer (EML) may exhibit higher electroluminescence (EL) efficiency compared to the one with the MPPO EML. Additionally, a slight difference in the bathochromic shift was observed between the PL spectra of MPPO and DPPO in both 10^{-5} M cyclohexane solutions and solid states. Hence, we can disregard the packing effects in the OLED devices. We conducted cyclic voltammetry (CV) to measure the oxidation potentials of the emitting materials, aiming to understand the impact of molecular symmetry on their energy band structure. The highest occupied molecular orbital (HOMO) energy levels (E_{HOMO}), determined from the onset potential of oxidation, were 5.2 and 5.3 eV for MPPO and DPPO, respectively, indicating a minor difference. However, the lowest unoccupied molecular orbital (LUMO) energy levels (E_{LUMO}), calculated by adding the optical bandgaps derived from the UV-vis spectra to the EHOMO values, were 2.2 and 2.5 eV, respectively. The symmetric A-D-A type molecule, DPPO, which features two electron-accepting groups on both sides, exhibited a higher electron affinity and a lower E_{LUMO} compared to the asymmetric D-A type molecule, MPPO, which has only one electron-accepting group. The reduced E_{LUMO} of DPPO is advantageous for enhancing its electron-capturing capability in the resulting OLED device. We also fabricated hole-only and electron-only devices based on both compounds and measured their current density as a function of the applied potential. However, we observed minimal differences in the charge-carrier mobility. The sole effect of introducing an additional electron-accepting group to DPPO was a decrease in the E_{LUMO} value.

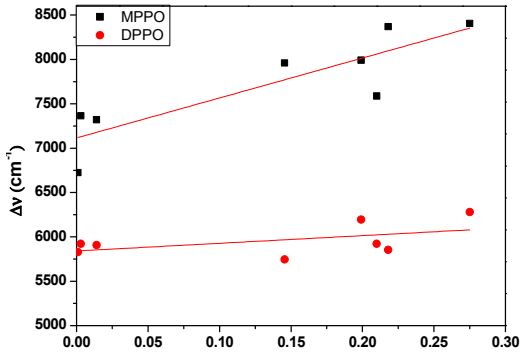

Figure 3. Dependence of the Stokes shift ($\Delta \nu$) of MPPO and DPPO as a function of orientational polarizability (Δf).

Table 3. Cavity Radius and Dipole Moment of the D-A Type Molecules

	* α	* μ_g (D)	μ_e (D)	$\triangle \mu$
MPPO	3.24	3.3	7.0	3.7
DPPO	3.24	2.5	4.1	1.6

3.3. Electroluminescence properties

We fabricated OLED devices utilizing a single EML of either MPPO

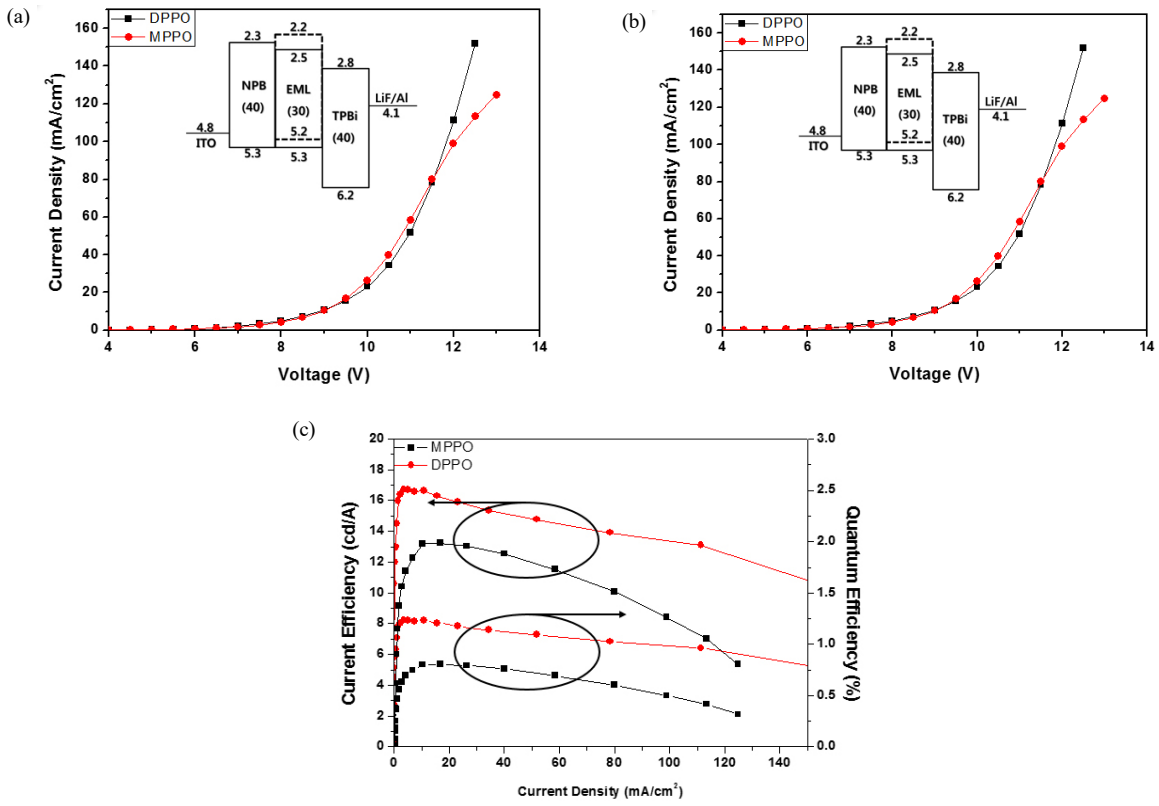

Figure 4. Current density-voltage-luminance (J-V-L) characteristics and efficiencies of the DA type molecule based OLEDs. (a) voltage vs. current density relations for the D-A type molecules based OLEDs. Inset is the energy level diagram of OLED devices based on MPPO (dashed line) and DPPO (solid line): ITO/ NPB (40 nm)/ EML (30 nm)/ TPBi (40 nm)/ LiF (1 nm)/ Al (100 nm), (b) voltage vs. luminescence characteristics. Inset indicate the EL spectra of OLED devices, (c) efficiencies for the D-A type molecules based OLEDs.

Table 4. Electroluminescent Data of the OLED Devices Based on the D-A Type Materials

	V_{on} (V)[a]	L_{max} (cd/m^2)[b]	η_C (cd/A)[b]	η_P (lm/W)[b]	EQE (%)[b]	$\lambda_{max,EL}$ (nm)
MPPO	4.5	3,300	4.2	1.8	1.5	500
DPPO	3.5	7,900	7.8	3.8	2.4	516

[a] measured at 1 cd/m^2 [b] measured at 100 cd/m^2

or DPPO, with a device structure of [ITO/N,N'-Bis(naphthalen-1-yl)-N,N'-bis(phenyl)benzidine (NPB, 10 nm)/emitting layer (EML, 30 nm)/2,2',2"-(1,3,5-Benzinetriyl)-tris(1-phenyl-1-H-benzimidazole) (TPBi, 40 nm)/LiF (1 nm)/Al (100 nm)]. The current density-voltage-luminance (J-V-L) characteristics are displayed in Figure 4, and the inset of Figure 4(a) presents the energy band diagram of the devices. NPB served as a hole-injection layer, and TPBi as an electron-transporting and hole-blocking layer. As summarized in Table 4, the turn-on voltages were 4.5 V and 3.5 V for the MPPO and DPPO devices, respectively, likely due to the difference in LUMO energy levels. The current efficiency of the DPPO-based device reached 7.8 cd/A, and the external quantum efficiency (EQE) was 2.4% at 100 cd/m², demonstrating significantly improved values compared to the MPPO-based device, which achieved 4.2 cd/A and 1.5%, respectively. EL efficiency is typically influenced by two factors: charge-carrier balance and the quantum yield of emitting materials[28, 42]. The OLED device with the symmetric DPPO emitter seems to have exhibited enhanced EL characteristics because the polarity of the emitting molecules changed minimally upon excitation. Additionally, the lower LUMO level of DPPO helped reduce the energy barrier for electron injection from the TPBi layer to the emitting layer, resulting in a better charge-carrier balance and a relatively smaller reduction in current efficiency at high current density.

4. Conclusions

We synthesized two D-A type emitting materials, DPPO and MPPO, with symmetric and asymmetric molecular geometries, respectively. These compounds possessed different excited-state dipole moments. Solvatochromic results indicated that the symmetric DPPO experienced a smaller change in dipole moment when excited, suggesting it would likely yield a higher quantum efficiency when used as the emitting lay-

er in an OLED device. The DPPO-based OLED device exhibited a current efficiency of 7.8 cd/A and an external quantum efficiency (EQE) of 2.4% at 100 cd/m², demonstrating approximately double the performance compared to the MPPO-based device. This indicates that the molecular symmetry of the D-A type emitting materials played a crucial role in the smaller dipole moment change and the higher quantum yield of emitting materials. Furthermore, the lower LUMO level of DPPO reduced the energy barrier for electron injection, resulting in better charge-carrier balance and a relatively smaller reduction in current efficiency at high current density.

Acknowledgements

This research was supported by the Basic Science Research Program through the National Research Foundation of Korea (NRF) funded by the Ministry of Education (2020R1A6A1A03048004). This work was supported by the GRRC program of Gyeonggi province. (GRRC KYUNGHEE2023-B01), Development of ultra-fine process materials based on the sub-nanometer class for the next-generation semiconductors]. This work was supported by the Korea Basic Science Institute (KBSI) National Research Facilities & Equipment Center (NFEC) grant funded by the Korea government (Ministry of Education). (No.2020R1A6C103B085 & No. 2019R1A6C1010052).

References

1. E. Mondal, W.-Y. Hung, H.-C. Dai, and K.-T. Wong, Fluorene-based asymmetric bipolar universal hosts for white organic light emitting devices, *Adv. Funct. Mater.*, **23**, 3096-3105 (2013).
2. H. D. Pham, L. Xianqiang, W. Li, S. Manzhos, A. K. K. Kyaw, and P. Sonar, Organic interfacial materials for perovskite-based optoelectronic devices, *Energy Environ. Sci.*, **12**, 1177-1209 (2019).
3. X. Xu, L. Yu, Q Peng, Recent Avances in Wide Bandgap Polymer Donors and Their Applications in Organic Solar Cells, *Chin. J. Chem.,* **39**, 24-254 (2021).
4. H. M. Heitzer, T. J. Marks, and M. A. Ratner, Molecular donor–bridge–acceptor strategies for high-capacitance organic dielectric materials, *J. Am. Chem. Soc.*, **137**, 7189-7196 (2015).
5. B. Lu, Y. Huang, Z. Zhang, H. Quan, and Y. Yao, Organic conjugated small molecules with donor–acceptor structures: Design and application in the phototherapy of tumors, *Mater. Chem. Front.*, **6**, 2968-2993 (2022).
6. Y. Li, J.-Y. Liu, Y.-D. Zhao, and Y.-C. Cao, Recent advancements of high efficient donor–acceptor type blue small molecule aapplied for OLEDs, *Mater. Today.*, **20**, 258-266 (2017).
7. T. Yang, Z. Cheng, Z. Li, J. Liang, Y. Xu, C. Li, and Y. Wang, Improving the efficiency of red thermally activated delayed fluorescence organic light-emitting diode by rational isomer engineering, *Adv. Funct. Mater.*, **30**, 2002681 (2020).
8. T. C. Yiu, P. Gnanasekaran, W.-L. Chen, W.-H. Lin, M.-J. Lin, D.-Y. Wang, C.-W. Lu, C.-H. Chang, and Y. J. Chang, Multifaceted sulfone−carbazole-based D−A−D materials: A blue fluorescent emitter as a host for phosphorescent OLEDs and triplet −triplet annihilation up-conversion electroluminescence, *ACS Appl. Mater. Interfaces*, **15**, 1748-1761 (2023).
9. L. Xue, J. He, X. Gu, Z. Yang, B. Xu, and W. Tian, Efficient bulk-heterojunction solar cells based on a symmetrical D-Π-A-Π-D organic dye molecule, *J. Phys. Chem. C*, **113**, 12911-12917 (2009).
10. K. H. Choi, J. M. Kim, W. J. Chung, and J. Y. Lee, Effects of substitution position of carbazole-dibenzofuran based high triplet energy hosts to device stability of blue phosphorescent organic light-emitting diodes, *Molecules*, **26**, 2804 (2021).
11. J. Lee, K. Shizu, H. Tanaka, H. Nomura, T. Yasuda, and C. Adachi, Oxadiazole-and triazole-based highly-efficient thermally activated delayed fluorescence emitters for organic light-emitting diodes, *J. Mater. Chem. C*, **1**, 4599-4604 (2013).
12. Y. Li, X.-L. Li, D. Chen, X. Cai, G. Xie, Z. He, Y.-C. Wu, A. Lien, Y. Cao, and S.-J. Su, Design strategy of blue and yellow thermally activated delayed fluorescence emitters and their all-fluorescence white OLEDs with external quantum efficiency beyond 20%, *Adv. Funct. Mater.*, **26**, 6904-6912 (2016).
13. L. K. Noda and N. S. Gonçalves, Assignment of the electronic transition of phenothiazine radical cation in the visible regione a resonance Raman spectroscopy and theoretical calculation investigation, *J. Mol. Struct.*, **1191**, 253-258 (2019).
14. Z. Li, W. Li, C. Keum, E. Archer, B. Zhao, A. M. Z. Slawin, W. Huang, M. C. Gather, I. D. W. Samuel, and E. Zysman-Colman, 1,3,4-oxadiazole-based deep blue thermally activated delayed fluorescence emitters for organic light emitting diodes, *J. Phys. Chem. C*, **123**, 24772-24785 (2019).
15. S. Xiang, R. Guo, Z. Huang, X. Lv, S. Sun, H. Chen, Q. Zhang, and L. Wang, Highly efficient yellow nondoped thermally activated delayed fluorescence OLEDs by utilizing energy transfer between dual conformations based on phenothiazine derivatives, *Dyes Pigm.*, **170**, 107636 (2019).
16. S. Xiang, Z. Huang, S. Sun, X. Lv, L. Fan, S. Ye, H. Chen, R. Guo, and L. Wang, Highly efficient non-doped OLEDs using aggregation-induced delayed fluorescence materials based on 10-phenyl-10H-phenothiazine 5,5-dioxide derivatives, *J. Mater. Chem. C*, **6**, 11436-11443 (2018).
17. X.-H. Zhang, S. H. Kim, I. S. Lee, C. J. Gao, S. I. Yang, and K. H. Ahn, Synthesis, photophysical and electrochemical properties of novel conjugated donor-acceptor molecules based on phenothiazine and benzimidazole, *Bull. Korean Chem. Soc.*, **28**, 1389-1395 (2007).
18. R. Sreenivasulu, M. B. Tej, S. S. Jadav, P. Sujitha, C. G. Kumar, and R. R. Raju, Synthesis, anticancer evaluation and molecular docking studies of 2,5-bis(indolyl)-1,3,4-oxadiazoles, Nortopsentin analogues, *J. Mol. Struct.*, **1208**, 127875 (2020).
19. H. Shen, Y. Li, and Y. Li, Self-assembly and tunable optical properties of intramolecular charge transfer molecules, *Aggregate*, **1**, 57-68 (2020).
20. V. Gopia, S. Subbiahraja, K. Chemmanghattu, P. C. Ramamurthy, 2,3-di(2-furyl) quinoxaline bearing 3 -ethyl rhodanine and 1,3 indandione based heteroaromatic conjugated T-shaped push −pull chromophores: Design, synthesis, photophysical and non-linear optical investigations, *Dyes Pigm.*, **173**, 107887 (2020).
21. Y. Zhang, Y. Wang, C. Gao, Z. Ni, X. Zhang, W. Hude, and H. Dong, Recent advances in n-type and ambipolar organic semiconductors and their multi-functional applications, *Chem. Soc. Rev.*, **52**, 1331 (2023).

22. H. M. Diab, A. M. Abdelmoniem, M. R. Shaaban, I. A. Abdelhamid, and A. H. M. Elwahy, An overview on synthetic strategies for the construction of star-shaped molecules, *RSC Adv.*, **9**, 16606 (2019).
23. M. L. Wilde, J. Menz, C. LEder, and K. Kümmerer, Combination of experimental and in silico methods for the assessment of the phototransformation products of the antipsychotic drug/metabolite Mesoridazine, *Sci. Total Environ.*, **618**, 697-711 (2018).
24. Y.Yu, Z.Yu, Z.Ma, J. Jiang, and D. Hu, D-π-A-π-D-type Fluorophores based on Pyridal[2,1,3]thiadiazole acceptor with hybridized local and charge-transfer excited-state for high-efficiency OLEDs, *Dyes Pigm.*, **208**, 110868. (2022).
25. M. Soroceanu, C.-P. Constantin, and M.-D. Damaceanu, A straightforward synthetic strategy towards conjugated donor-acceptor naphthylimido-azomethines with tunable films morphologies and opto-electronic properties, *Prog. Org. Coat.,* **166**, 106785 (2022).
26. S. Sasaki, G. P. C. Drummen, and G. I. Konishi, Recent advances in twisted intramolecular charge transfer (TICT) fluorescence and related phenomena in materials chemistry, *J. Mater. Chem. C*, **4**, 2731-2743 (2016).
27. N. J. Turro, V. Ramamurthy, and J. C. Scaiano, *Modern Molecular Photochemistry of Organic Molecules*, 127, University Science Books, Sausalito (California), USA (2010).
28. C. Wang, W. Chi, Q. Qiao, D. Tan, Z. Xu, and X. Liu, Twisted intramolecular charge transfer (TICT) and twists beyond TICT: From mechanisms to rational designs of bright and sensitive fluorophores, *Chem. Soc. Rev.*, **50**, 12656-12678 (2021).
29. M. Sun, T. Li, M. Xie, H. Zhou, Q. Sun, D. Liu, Y. Pan, S. Zhang, W. Yang, and S. Xue, Highly efficient deep-blue electrofluorescence with optimized excited state composition and "hot-exciton" channel, *Dyes Pigm.*, **210**, 111002 (2023).
30. J. Kumsampao, C. Chaiwai, C. Sukpattanacharoen, P. Nalaoh, T. Chawanpunyawat, P. Chasing, S. Namuangruk, N. Kungwan, T. Sudyoadsuk, and V. Promarak, Solid-state fluorophores with combined excited-state intramolecular proton transfer-aggregation-induced emission as efficient emitters for electroluminescent devices, *Adv. Photonics Res.*, **3**, 2100141 (2022).
31. B. Valeur and M. N. Berberan-Santos, *Molecular Fluorescence: Principles and Applications*, 2nd ed., 53, John Wiley & Sons, Weinheim, Germany (2012).
32. X. Xiang, Y. Zhan, W. Yang, and F. Jin, Aggregation-induced emission and distinct mechanochromic luminescence based on symmetrical D-A-D type and unsymmetrical D-A type carbazole functionalized dicyanovinyl derivatives, *J. Lumin.*, **252**, 119287 (2022).
33. H. Liu, S. Yan, R. Huang, Z. Gao, G. Wang, L. Ding, Y. Fang, Single-benzene-based solvatochromic chromophores: color-tunable and bright fluorescence in the solid and solution states, *Chem. Eur. J.*, **25**, 16732-16739 (2019).
34. M.-L. Hebestreit, H. Lartian, C. Henrichs, R. Ku¨hnemuth, W. L. Meerts, and M. Schmitt, Excited state dipole moments and lifetimes of 2-cyanoindole from rotationally resolved electronic Stark spectroscopy, *Phys. Chem. Chem. Phys.*, 2**3**, 10196-10204 (2021).
35. C.-H. Chen, Y. Wang, T. Michinobu, S.-W. Chang, Y.-C. Chiu, C.-Y. Ke, and G.-S. Liou, Donor−acceptor effect of carbazole-based conjugated polymer electrets on photoresponsive flash organic field-effect transistor memories, *ACS Appl. Mater. Interfaces*, **12**, 6144-6150 (2020).
36. D. Kim, Y. J. Lee, D.-H. Ahn, J.-W. Song, J. Seo, and H. Lee, Peptoid-conjugated magnetic field-sensitive exciplex system at high and low solvent polarities, *J. Phys. Chem. Lett.*, **11**, 4668-4677 (2020).
37. M. Poddar, A. Cesaretti, E. Ferraguzzi, B. Carlotti, and R. Misra, Singlet and triplet excited-state dynamics of 3,7-bis(arylethynyl) phenothiazines: intramolecular charge transfer and reverse intersystem crossing, *J. Phys. Chem. C*, **124**, 17864-17878 (2020).

Authors

Hyun Gi Kim; Ph.D., Research Professor, Department of Chemical Engineering, Kyung Hee University, Yongin-si 17104, Korea; opti_people@khu.ac.kr

Young-Seok Baek; M.Sc., Researcher, Department of Chemical Engineering, Kyung Hee University, Yongin-si 17104, Korea; bys376@khu.ac.kr

Sung Soo Kim; Ph.D., Professor, Department of Chemical Engineering, Kyung Hee University, Yongin-si 17104, Korea; sungkim@khu.ac.kr

Sang Hyun Paek; Ph.D., Professor, Department of Chemical Engineering, Kyung Hee University, Yongin-si 17104, Korea; shpaek@khu.ac.kr

Young Chul Kim; Ph.D., Professor, Department of Chemical Engineering, Kyung Hee University, Yongin-si 17104, Korea; kimyc@khu.ac.kr